

# Analysis of Vertical Ground Motion / Phase Motion Near Fault Records in JAPAN and Its Application to Simulation of Vertical Ground Motion



**T. HARADA & M. NAKAMURA**

*Dept. of Civil and Environmental Engineering, University of Miyazaki, Japan*

**N. KANAI**

*Disaster Prevention Management Dept., Oita Works, Nippon Steel Corporation, Oita, Japan*

**15 WCEE**  
LISBOA 2012

**T. NONAKA, Y. KODAMA & H. MOTOHASHI**

*Earthquake Engineering Research Center Inc., University of Miyazaki, Miyazaki, Japan*

## SUMMARY:

In this paper, the characteristics of the vertical component of the ground motion recorded near the source in inland earthquakes occurred in Japan are studied. The curves for the Fourier spectral amplitude ratio ( $V/H$ ) of vertical to horizontal components are analyzed and summarized in terms of the mean and standard deviation of them for three types of surface soil conditions. Also the characteristics of the vertical ground motions synthesized using the thrust (reverse) kinematic source models are compared with the observed curves for the  $V/H$  spectral ratio as well as the records at the KiK-net IWATH25 station during the 2008 Iwate-Miyagi Nairiku earthquake in Japan. Finally, an engineering method to simulate vertical ground motion is presented using the proposed  $V/H$  spectral ratio and the concept of phase motion. The simulated vertical ground motions using both the engineering method and the seismological method are compared with the records.

*Keywords: Vertical ground motion, Phase motion, Near field ground motion, Engineering method of simulation of vertical ground motion, Analysis of ground motions at the KiK-net IWATH25 station during the 2008 Iwate-Miyagi Nairiku earthquake in Japan*

## 1. INTRODUCTION

Compared with knowledge of the relationships between the horizontal ground motions and the nonlinear dynamic structural response behavior, we have still known a little the effect of the vertical ground motions on the nonlinear dynamic structural response behavior. Most seismic codes worldwide ignore it or include the vertical response spectral value as 50~70% of the horizontal response spectral value. However, the recent studies have been suggesting that the effect of the vertical ground motion can be significant for the response of bridges near the faults (Gülerce and Abrahamson, 2010, Kodama and Harada et al. 2011, 2012). And also, with the accumulation of the near field (source) strong motion records in Japan, many strong ground motion records, in which the vertical component is greater than the horizontal component, have been observed. An example of these records is the record at the KiK-net IWATH25 station during the 2008 Iwate-Miyagi Nairiku earthquake in Japan where the peak acceleration of the vertical component at the surface record was  $3,866 (cm/s^2)$  larger than the  $1,435 (cm/s^2)$  of the horizontal component. From viewpoint of the source (fault) model, the normal and thrust (reverse) faults tend to provide large vertical motions including permanent vertical ground deformations due to those fault ruptures.

In the first part of this paper, the characteristics of the vertical component of the ground motion recorded near the source in inland earthquakes occurred in Japan are studied. And also, the characteristics of the phase ground motion, which is defined by putting its Fourier spectral amplitude to be unit in the frequency range considered, are examined. In this study, the curves for the Fourier spectral amplitude ratio ( $V/H$ ) of vertical to horizontal component are analyzed and summarized in terms of the mean and standard deviation of them for three types of surface soil conditions. Also the characteristics of the vertical ground motions synthesized using the thrust (reverse) kinematic source models are compared with the observed characteristics of the curves for the Fourier spectral amplitude

ratio ( $V/H$ ) of vertical to horizontal component as well as the records at the KiK-net IWATH25 station during the 2008 Iwate-Miyagi Nairiku earthquake in Japan.

In the second part, for the purpose of engineering application, an engineering method to simulate the vertical ground motion is presented using the proposed Fourier spectral amplitude ratio ( $V/H$ ) and the concept of phase motion without using a seismological source model. The simulated vertical ground motion using both an engineering method and a seismological method are compared with the records, in order to demonstrate an engineering capability of the proposed simulation methods of vertical ground motion with the permanent ground deformation due to the fault ruptures near a fault.

## 2. CHARACTERISTICS OF VERTICAL GROUND MOTIONS RECORDED NEAR THE SOURCES IN THE INLAND EARTHQUAKES OCCURRED IN JAPAN

### 2.1. Selection of the Dataset and the Near Field Ground Motions Recorded at the KiK-net IWATH25 Station during the 2008 Iwate-Miyagi Nairiku Earthquake

This study uses the strong acceleration motions with peak acceleration larger than  $100 (cm/s^2)$  on the surface of ground recorded by the 28 K-NET stations within the shortest distance of 20 km from the 9 inland earthquake faults of  $M_{JMA}$  6.2-7.3 occurred in Japan during 2000 to 2008. Table 2.1 summarizes the characteristics of the 9 inland earthquakes and the 28 K-NET stations names and their surface soil conditions of 3 types (Type I : rock ( $T_G < 0.2 (s)$ ), Type II: medium soil ( $0.2 (s) < T_G < 0.6 (s)$ ), and Type III: soft soil ( $T_G > 0.6 (s)$ )) classified by the Japanese seismic design standard of bridges for road and highway. Herein,  $T_G$  means the predominant period of the surface ground at the recording stations.

Figure 2.1 shows the location of the fault projection and epicenter of the 2008 Iwate-Miyagi Nairiku earthquake ( $M_{JMA}$  7.2). And also in this figure, the location of the 5 K-NET stations and the Ichinoseki Nishi station (IWTH25; Soil condition is a type I (rock)) of KiK-net, which is the closest station of the fault, are indicated. The ground surface accelerations recorded at the station of IWTH25 are shown in Figure 2.2, indicating the very larger vertical acceleration of  $3,866 (cm/s^2)$  than the EW component of horizontal acceleration of  $1,435 (cm/s^2)$

**Table 2.1.** Summary of the Characteristics of the 9 Inland Earthquakes and the 28 K-NET Station Names and Their Soil Conditions within the Shortest Distance of 20 km from the Faults used in This Study

Earthquake Name (Year/Month/Day)	$M_{JMA}$	Type of Fault	Name of K-NET Stations and Soil Conditions within the Shortest Distance of 20 Km from the Fault
Tottori-Ken Seibu (2000/10/06)	7.3	Strike Slip	TTR007 (Type II), TTR008 (Type III), TTR009 (Type II), SMN015 (Type II)
Geiyo (2001/03/24)	6.4	Normal	HRS019 (Type III), EHM007 (Type II)
Off Miyagi-Ken (2003/05/26)	7.0	Thrust	MYG001 (Type II), MYG002 (Type I), IWT008 (Type I)
North Miyagi-Ken (2003/07/23)	6.2	Thrust	MYG007 (I type), MYG010 (III type), MYG012 (III type)
Niigata Tyuetsu (2004/10/23)	6.8	Thrust	NIG017 (Type II), NIG019 (Type II), NIG020 (Type II), NIG021 (Type II)
Off West Fukuoka-Ken (2005/03/20)	7.0	Strike Slip	FKO006 (Type III), FKO007 (Type II)
Off Noto Peninsula (2007/03/25)	6.9	Thrust + Strike Slip	ISK003 (Type I), ISK005 (Type III), ISK006 (Type I)
Off Niigata Tyuetsu (2007/07/16)	6.8	Thrust	NIG016 (Type II), NIG018 (Type III)
Iwate-Miyagi Nairiku (2008/06/14)	7.2	Thrust	AKT023 (Type II), IWT010 (Type I), IWT011 (Type II), MYG004 (Type I), MYG005 (Type I)

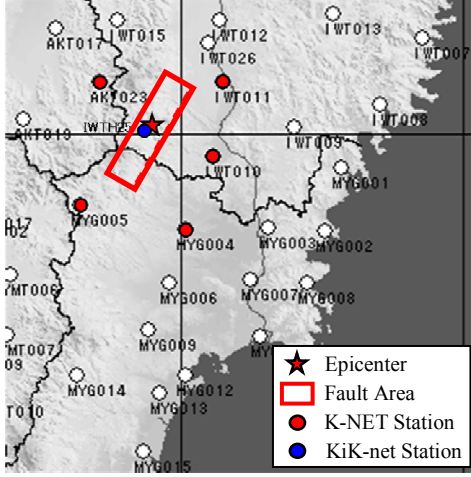


**Figure 2.1.** The location of the fault projection and epicenter of the 2008 Iwate-Miyagi Nairiku earthquake ( $M_{JMA}7.2$ ) and of the 5 K-NET stations and the Ichinoseki station (IWT25)

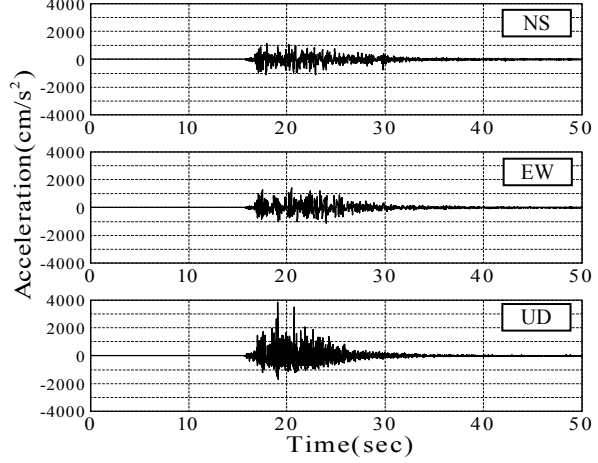


**Figure 2.2.** Ground surface acceleration motions recorded at the closest station of IWT25 during the 2008 Iwate-Miyagi Nairiku earthquake ( $M_{JMA}7.2$ )

## 2.2. Model Results of the Fourier Spectral Amplitude Ratio (V/H) of Vertical to Horizontal Component

Using the acceleration motions on the ground surface recorded by the 28 K-NET stations within the shortest distance of 20 km from the 9 inland earthquake faults indicated in Table 2.1, the Fourier spectral amplitude ratio ( $V/H = |V(T)|/|H(T)|$ ;  $T(s)$  = period of ground motion) is calculated for each soil condition by the use of the smoothing of Parzen window with the band width of 0.1 (Hz), and then the mean value and standard deviation of the  $V/H$  are obtained for each soil condition. The number of recording stations for each type of soil condition are the 8 stations for the Type I, 13 stations for the Type II, and 7 stations for the Type III. In this study, the horizontal component  $|H(T)|$  is calculated by the root sum square (RSS) (square root of sum of squares) of the NS and EW components.

Figure 2.3 to Figure 2.5 show the results of  $V/H$  for each type of soil conditions (Type I, Type II, and Type III). In these figures, the tree values of  $V/H$  ;[the mean] value, [mean + standard deviation] value ,and [mean + 2 times standard deviation] value ,are plotted. To approximate and model these characteristics of  $V/H$  obtained from the recorded near field ground motions, the following equations consisting of three lines in the logarithmic figure are adopted, and also the values of these equations are indicated by the three lines in Figure 2.3 to Figure 2.5.

For  $V/H$  of Type I soil condition (Rock):

$$E \left[ \frac{|V(T)|}{|H(T)|} \right] + m\sigma_{FI}$$

$$= \begin{cases} 1.4 + m\sigma_{FI} & 0.03 \leq T \leq 0.06 \\ (1.4 + m\sigma_{FI}) \left( \frac{0.06}{T} \right)^2 & 0.06 \leq T \leq 0.13 \\ (1.4 + m\sigma_{FI}) (0.46)^2 & 0.13 \leq T \leq 5 \end{cases} \quad (2.1)$$

where the mean of  $V/H$  is given by  $m=0$ ,  $\sigma_{FI} = 0.7$ .

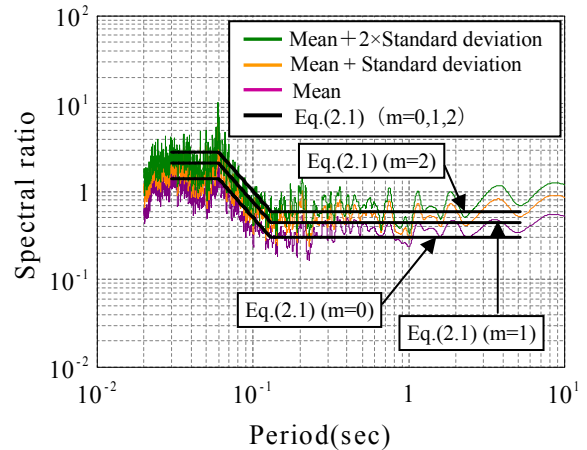


**Figure 2.3.** The  $V/H$  of recorded motions for Type I soil condition and its approximation

For  $V/H$  of Type II soil condition (Medium soil) :

$$E \left[ \frac{|V(T)|}{|H(T)|} \right] + m\sigma_{FII}$$

$$= \begin{cases} 1.4 + m\sigma_{FII} & 0.03 \leq T \leq 0.09 \\ (1.4 + m\sigma_{FII}) \left( \frac{0.09}{T} \right)^{1.5} & 0.09 \leq T \leq 0.25 \\ (1.4 + m\sigma_{FII}) (0.36)^{1.5} & 0.25 \leq T \leq 5 \end{cases} \quad (2.2)$$

where  $\sigma_{FII} = 1.0$ .

For  $V/H$  of Type III soil condition (Soft soil) :

$$E \left[ \frac{|V(T)|}{|H(T)|} \right] + m\sigma_{FIII}$$

$$= \begin{cases} 2.3 + m\sigma_{FIII} & 0.03 \leq T \leq 0.09 \\ (2.3 + m\sigma_{FIII}) \left( \frac{0.09}{T} \right) & 0.09 \leq T \leq 1.0 \\ (2.3 + m\sigma_{FIII}) (0.09) & 1.0 \leq T \leq 5 \end{cases} \quad (2.3)$$

where  $\sigma_{FIII} = 1.3$ .

In the above approximations of Eq. (2.1) to Eq. (2.3), the range of period  $T$  (s) of ground motion is to be 0.03 (s) to 5 (s). As a matter of course, the above approximations should be changed by accumulating the near fault ground motions.

### 3. COMPARISON OF GROUND MOTION DISPLACEMENTS AND $V/H$ OF THE 2008 IWATE-MIYAGI NAIRIKU EARTHQUAKE ( $M_{JMA}$ 7.2) IN JAPAN WITH THE SIMULATED RESULTS BY A KINEMATIC SOURCE MODEL

Because the very close fault strong ground motions are limited, a theoretical simulation method using a seismological model is an alternative tool to capture the nature of the very close fault strong ground motions. In this chapter, to demonstrate the capability of the theoretical simulation method using a kinematic source model, the simulated ground motion displacements and  $V/H$  ratio are compared with those of the records at the Ichinoseki Nishi station (IWTH25; Soil condition is a type I (rock)) of KiK-net, which is the closest station of the fault of the 2008 Iwate-Miyagi Nairiku earthquake ( $M_{JMA}$  7.2). As a theoretical simulation method, this study uses the stiffness matrix method for the multi-layered half space model and the kinematic source model (Harada and Wang, 2005, Wang, 2006). The ground motions in this method are computed by the 3 fold Fourier transform of the displacements in frequency wave number domain that can be obtained by solving the stiffness matrix equation for the source and multi-layered half space system.

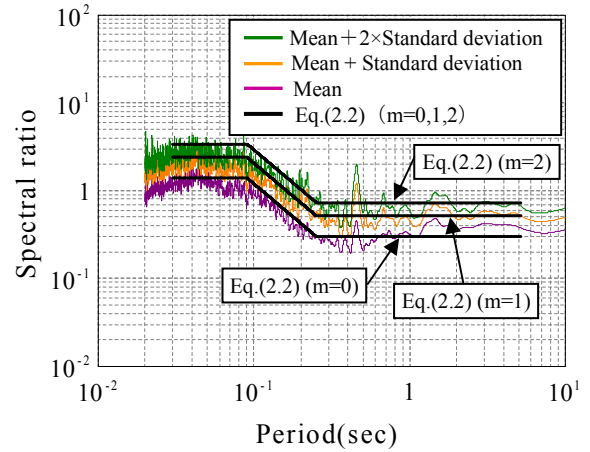


**Figure 2.4.** The  $V/H$  of recorded motions for Type II soil condition and its approximation

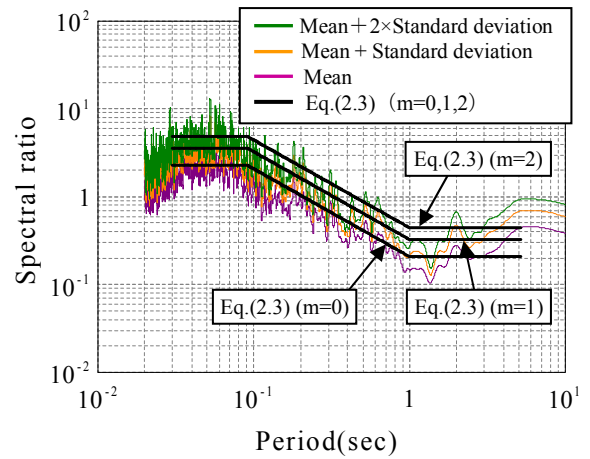


**Figure 2.5.** The  $V/H$  of recorded motions for Type III soil condition and its approximation

By referring the inversion results of the source model by Suzuki et al. (2010), the closest asperity to the Ichinoseki Nishi station (IWTH25) of KiK-net is used as an initial source model in this study. Table 3.1 indicates the kinematic source model parameters, and Table 3.2 the thickness of a surface layer on half space and their elastic properties used in this study. Figure 3.1 shows the source dimensions and the location of the Ichinoseki Nishi station (IWTH25).

**Table 3.1.** Thrust Fault Parameters used in Simulation

	Fault ①	Fault ②
Seismic Moment $M_0$ (N-m)	$1.48 \times 10^{18}$	$5.55 \times 10^{17}$
Length $L$ (km)	5.6	2.1
Width $W$ (km)	7.7	
Rupture Velocity $v_r$ (km/s)	2.8	
Strike Angle $\phi$ ( $^\circ$ )	209.0	
Dip Angle $\delta$ ( $^\circ$ )	50.0	48.0
Slip Direction $\lambda$ ( $^\circ$ )	104.0	

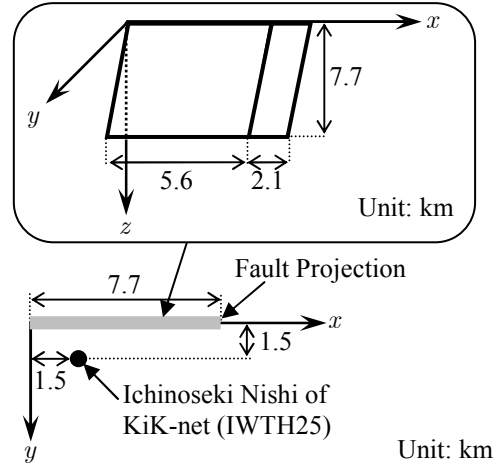


**Table 3.2.** Thickness of Surface Layer and Elastic Properties of Layered Half Space

	Surface Layer	Half Space
Thickness (km)	0.4	—
P Wave Velocity (km/s)	3.0	6.0
S Wave Velocity (km/s)	1.8	3.5
Density ( $kg/m^3$ )	2300	2800
Q Value	150	400

**Figure 3.1.** The source dimensions and the location of the Ichinoseki Nishi Station (IWTH25) of KiK-net.

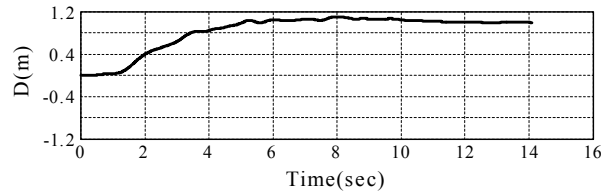


**Figure 3.2.** The source slip time function used in the simulation.

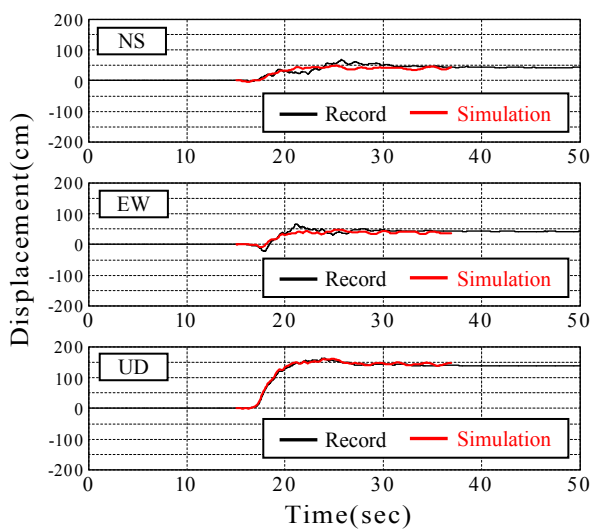


**Figure 3.3.** Comparison of the simulated ground displacements with those recorded at the Ichinoseki Nishi Station (IWTH25) of KiK-net

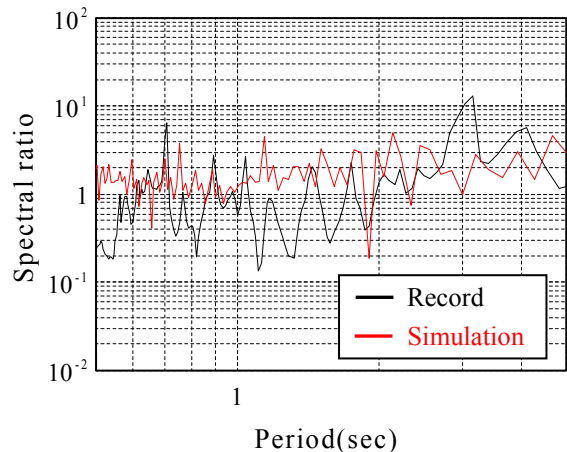


**Figure 3.4.** Comparison of the  $V/H$  ratio of the simulation with that of the recorded ground displacements (EW component is used as horizontal ground displacement)

By fixing the source parameters in Table 3.1, and the thickness of surface layer and elastic properties of layered half space in Table 3.2, the slip time function of the fault is adjusted so that the simulated ground displacements in frequency domain is similar to those calculated in the frequency domain using the recorded ground motion accelerations at the Ichinoseki Station (IWTH25) of KiK-net. The slip time function finally adopted in this study is shown in Figure 3.2. In the simulation, the longer period of ground motion displacements than that of 0.5 (s) is considered.

Figure 3.3 shows the results of comparing the simulated ground displacements with those recorded at the Ichinoseki Nishi station (IWTH25), indicating that the theoretical simulation method using the stiffness matrix method for the kinematic source and multi-layered half space system is an effective tool to capture the nature of the very close fault strong ground motions with the permanent ground deformation due to the thrust fault.

The  $V/H$  ratio of the simulated vertical to EW component of horizontal ground motion is compared with that of the recorded ground motions, and shown in Figure 3.4. In the range of period longer than 0.5 (s), the  $V/H$  ratio of the simulated ground motions is also similar to that of the recorded ground motions, also indicating that the theoretical simulation method can be used to complement the characteristics such as the  $V/H$  ratio of the ground motions in very close fault rupture. For example, the effects of the type of faults as well as the thickness of surface layers and the elastic properties of layered half space on the  $V/H$  ratio of very near source ground motions can be quantified using the theoretical simulation method.

#### 4. AN ENGINEERING METHOD OF SIMULATION OF VERTICAL GROUND MOTION USING THE $V/H$ RATIO AND THE CONCEPT OF PHASE MOTION

##### 4.1. The Concept of Phase Motion

The Fourier transform of a causal time function  $f(t)$  is given by Eq. (4.1).

$$F(\omega) = \int_0^{\infty} f(t)e^{i\omega t} dt \quad (4.1a)$$

where,

$$f(t) = \begin{cases} 0 & t < 0 \\ f(t) & 0 \leq t < \infty \end{cases} \quad (4.1b)$$

The Fourier spectrum is also expressed as the Fourier amplitude spectrum times the phase spectrum,

$$F(\omega) = |F(\omega)|e^{-i\theta(\omega)} \quad (4.2)$$

The phase motion of a causal time function  $f(t)$  is defined such that,

$$p(t) = \frac{1}{2\pi} \int_{-\infty}^{\infty} e^{-i(\omega t + \theta(\omega))} d\omega \quad (4.3)$$

where  $p(t)$  is the phase motion of a causal time function  $f(t)$ . The phase motion defined by Eq. (4.3) is corresponding to the inverse Fourier transform of the unit Fourier spectrum amplitude ( $|F(\omega)| = 1$ )

with the phase spectrum ( $e^{-i\theta(\omega)}$ ).

As an example of the phase motion of a causal time function  $f(t)$ , the vertical ground acceleration motion recorded at the closest station of IWTH25 during the 2008 Iwate-Miyagi Nairiku earthquake ( $M_{JMA}7.2$ ), which is shown in Figure 2.2, is used as a causal time function  $f(t)$ . The upper two figures of Figure 4.1 show the vertical ground acceleration motion as the causal time function  $f(t)$ , and second figure from the top is the phase vertical motion defined by Eq. (4.3) of the causal time function  $f(t)$ . It is observed from the second figure that the phase motion defined by Eq. (4.3) is not a causal time function, because it is exhibiting the small ground motion before the time (16.0 (s) in this figure) arriving the seismic wave motions.

To improve the nature of the non causal time function of the phase motion defined by Eq. (4.3), the smoothing of Parzen window with a band width is introduced to the Fourier amplitude spectrum, and then the improved phase motion is computed by the inverse Fourier transform of the approximate unit

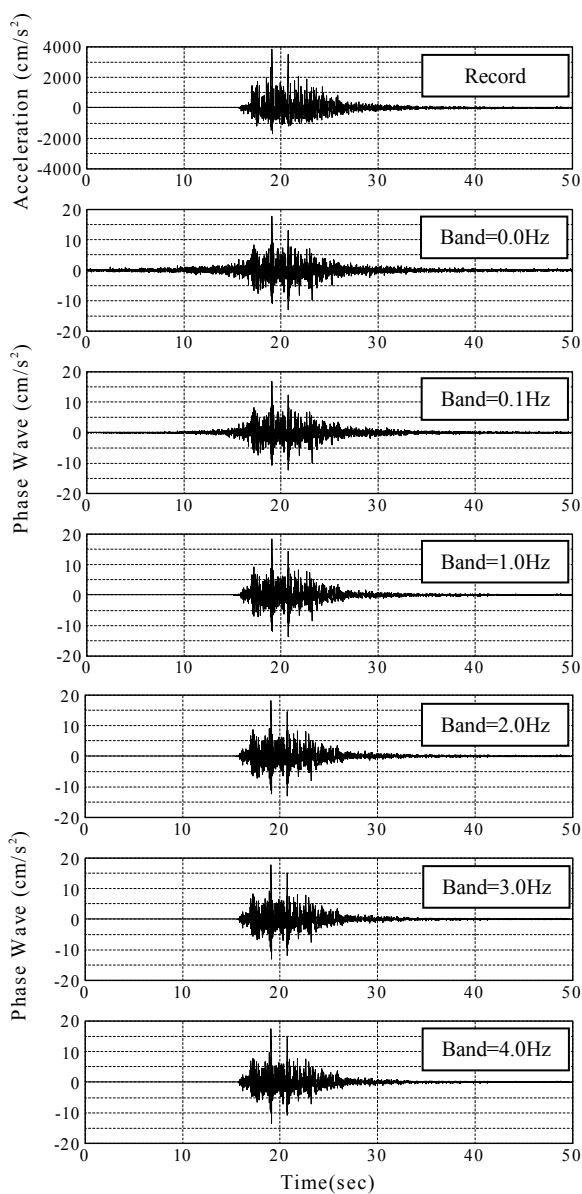


**Figure 4.1.** Vertical acceleration motion at IWTH25 (top figure) and its phase motion (the second figure, Band=0 (Hz)), and the modified phase motions (the third to the last figures, Band=0.1 (Hz) to 4.0 (Hz))

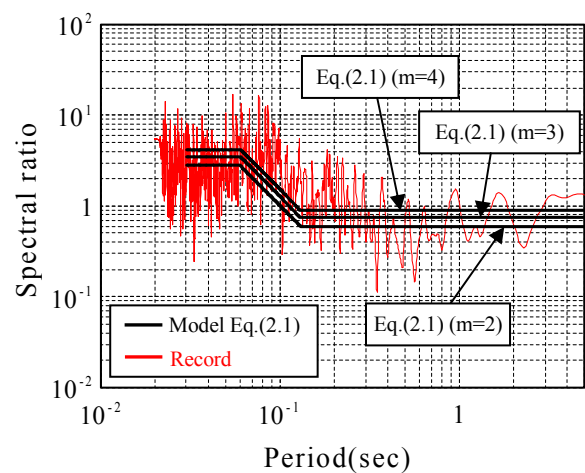


**Figure 4.2.** Comparison of the V/H ratio of the acceleration motions at IWTH25 with that of the Eq. (2.1)

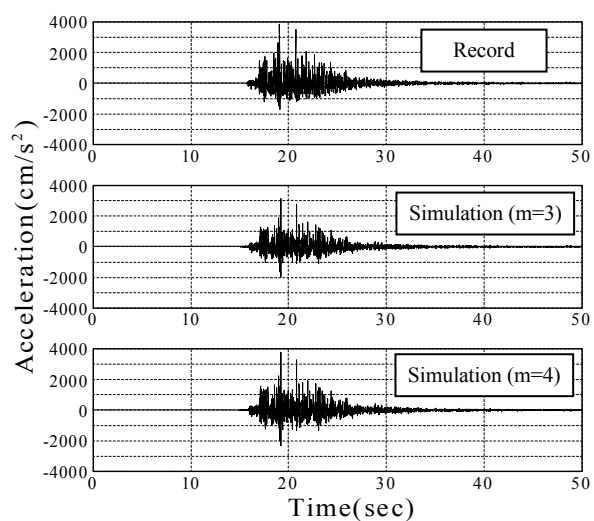


**Figure 4.3.** Comparison of the vertical acceleration motion at IWTH25 (top figure) with those of simulation using  $m=3$  and  $4$  in Eq. (2.1)

Fourier spectrum amplitude ( $|F(\omega)| / |\tilde{F}(\omega)|$ ) with the phase spectrum ( $e^{-i\theta(\omega)}$ ). Herein,  $|\tilde{F}(\omega)|$  means the smoothed Fourier spectrum amplitude.

Figure 4.1 shows the influence of the band width (Band = 0 (Hz), 0.1 (Hz), 1.0 (Hz), 2.0 (Hz), 3.0 (Hz), 4.0 (Hz)) of the smoothing of Parzen window on the improvement of the causality of the phase motion. The band width of 1.0 (Hz) may be the best one, because the larger band width (2.0 (Hz), 3.0 (Hz), 4.0 (Hz)) changes slightly the amplitude of the improved phase motion.

#### 4.2. An Engineering Simulation Method of Vertical Ground Motion using V/H ratio and Phase Motion

In this section, an engineering simulation method and a numerical example of the vertical ground motion is presented, for the condition that an appropriate phase motion of vertical ground motion (for example, the big earthquake ground motions caused severe damages) and the horizontal ground motions for seismic design are given. The vertical ground acceleration motion is computed by the following equations.

$$a_V(t) = \frac{1}{2\pi} \int_{-\infty}^{\infty} A_V(\omega) e^{-i\omega t} d\omega \quad (4.4)$$

in which,  $A_V(\omega)$  is the Fourier spectrum of vertical ground motion, and frequency  $\omega$  is related with the period  $T$  as  $\omega = 2\pi / T$ . The Fourier spectrum  $A_V(\omega)$  is given by,

$$A_V(\omega) = \left( E \left[ \frac{|V(\omega)|}{|H(\omega)|} \right] + m\sigma_{FJ} \right) \left[ \tilde{H}_D(\omega) \left( \frac{F_V(\omega)}{\tilde{F}_V(\omega)} \right) \right] \quad (4.5)$$

where, the first item of right hand side (RHS) of Eq. (4.5) is the approximate or modelled characteristics of  $V/H$  given by Eq. (2.1) to Eq. (2.3) for each soil condition. The second item of RHS of Eq. (4.5) means the smoothed Fourier spectrum amplitude of a given horizontal ground motion used in seismic design. The third item of RHS of Eq. (4.5) expresses the approximate phase spectrum of a given vertical ground motion that is approximately a causal time function.

As a numerical example of the engineering simulation of vertical ground motion using Eq. (4.4) and Eq. (4.5), the vertical ground motion recorded at the station IWTH25 (Soil condition is the Type I (rock)) of KiK-net, which is the closest station of the fault of the 2008 Iwate-Miyagi Nairiku earthquake ( $M_{JMA}7.2$ ) is simulated. In the simulation, Eq. (2.1) is used as the  $V/H$  ratio in rock site, and the NS component of recorded acceleration motion at the station IWTH25 is used as the smoothed Fourier spectrum amplitude of a given horizontal ground motion used in seismic design. As the approximate phase spectrum, the vertical component of ground acceleration motion at the station IWTH25 is used in this numerical example. The smoothing of Parzen window with a band width of 1.0 (Hz) is used for the smoothing of the Fourier spectrum amplitude in Eq. (4.5).

Figure 4.3 shows the simulated vertical ground accelerations in the range of period 0.03 (s) to 5 (s) for the values of  $m=3$ , and 4 in Eq. (2.1), by comparing with the vertical acceleration ground motions recorded at the very close station IWTH25 from the fault during the 2008 Iwate-Miyagi Nairiku earthquake ( $M_{JMA}7.2$ ). It is observed from Figure 4.3 that the simulated vertical ground motions are very similar to the recorded vertical ground motion when the values of [mean + 3 × standard deviation] or [mean + 4 × standard deviation] as the model of  $V/H$  ratio given by Eq. (2.1) are used, without using the value of [mean]. as the model of  $V/H$  ratio in Eq. (2.1), because the recorded vertical ground motion used in this numerical example is the record at the very close station from the fault.

## 5. CONCLUSIONS

The characteristics of the vertical component of the strong ground motion with the peak acceleration larger than 100 ( $cm/s^2$ ) on the surface of ground recorded by the 28 K-NET stations within the shortest distance of 20 km from the 9 inland earthquake faults of  $M_{JMA}$  6.2-7.3 occurred in Japan during 2000 to 2008, are studied in this paper, from view points of the empirical method, the theoretical simulation method on the basis of a seismological model, and the engineering simulation method using a concept of phase motion and the modelled Fourier spectral amplitude ratio ( $V/H$ ) of vertical to horizontal component of ground motions. The followings are the conclusions of this study.

- (1) The Fourier spectral amplitude ratio ( $V/H$ ) in the range of period of 0.03 (s)-5 (s) is modelled as the simple Eqs. (2.1), (2.2), and (2.3) for three soil conditions (Type I (rock), Type II (medium soil), and Type III (soft soil)) in which the mean value and the standard deviation of the  $V/H$  ratio are taken into account for in the modelled equations.
- (2) As a theoretical simulation method using a seismological model, this study uses the stiffness matrix method for the multi-layered half space and the kinematic source model for the simulation of ground displacement motions at the very close station IWTH25 during the 2008 Iwate-Miyagi Nairiku earthquake ( $M_{JMA}$ 7.2) in Japan, and it is found that the theoretical simulation method is an effective tool to simulate the ground displacement motions including the permanent ground deformation near a fault.
- (3) An engineering simulation method of vertical ground motion is also presented for the condition that an appropriate phase motion of vertical ground motion (for example, the big earthquake ground motions caused severe damages) and the horizontal ground motions for seismic design are given. In this method, the Fourier spectral amplitude ratio ( $V/H$ ) modelled in this study and the concept of the phase motion are used.

## ACKNOWLEDGEMENT

We are very indebted to the seismograms from the National Research Institute for Earth Science and Disaster Prevention (K-NET and KiK-net).

## REFERENCES

- Gülerce, Z. and Abrahamson, N. A. (2008). Vector-valued probabilistic seismic hazard assessment for the effects of vertical ground motions on the seismic response of highway bridges. *Earthquake Spectra* **26**: 999-1016.
- Harada, T. and Wang, H. (2005). Wave motion simulation method for multi-layered half space and kinematic source model. *ZISIN, Journal of the Seismological Society of Japan* **57**: 387-392.
- Kodama, Y., Harada, T., Nonaka, T., Nakamura, M. and Usami, T. (2011). Seismic behavior of a steel truss bridge near a thrust fault. *Journal of Structural Engineering, JSCE*, **57A**: 454-466.
- Kodama, Y., Harada, T., Nonaka, T., Nakamura, M. and Usami, T. (2012). Response characteristics and seismic reinforcement methods of a steel arch bridge near the faults. *Journal of Structural Engineering, JSCE*, **58A**: 436-447.
- Suzuki, W., Aoi, S. and Sekiguchi, H. (2010). Rupture process of the 2008 Iwate-Miyagi nairiku, Japan, Earthquake derived from near-source strong motion records. *Bulletin of the Seismological Society of America* **100, No.1**: 256-266.
- Wang, H. (2006). Theoretical method for characterization of near fault wave motion and response of extended structures. *University of Miyazaki Academic Repository*, <http://hdl.handle.net/10458/674>.